APL Materials

RESEARCH ARTICLE | OCTOBER 02 2013

# Scanning transmission electron microscopy investigations of self-forming diffusion barrier formation in Cu(Mn) alloys on $SiO_2$ FREE

J. G. Lozano; J. Bogan; P. Casey; A. P. McCoy; G. Hughes; P. D. Nellist



*APL Mater.* 1, 042105 (2013)
https://doi.org/10.1063/1.4822441

APL MATERIALS **1**, 042105 (2013)

# Scanning transmission electron microscopy investigations of self-forming diffusion barrier formation in Cu(Mn) alloys on $SiO_2$

J. G. Lozano,[1] J. Bogan,[2] P. Casey,[2] A. P. McCoy,[2] G. Hughes,[2] and P. D. Nellist[1]
[1]*Department of Materials, University of Oxford, Parks Road, OX13PH Oxford, United Kingdom*
[2]*School of Physical Sciences, Dublin City University, Glasnevin, Dublin 2, Dublin, Ireland*

(Received 4 July 2013; accepted 31 August 2013; published online 2 October 2013)

Scanning transmission electron microscopy in high angle annular dark field mode has been used to undertake a characterisation study with sub-nanometric spatial resolution of the barrier formation process for a Cu(Mn) alloy (90%/10%) deposited on $SiO_2$. Electron energy loss spectroscopy (EELS) measurements provide clear evidence for the expulsion of the alloying element to the dielectric interface as a function of thermal annealing where it chemically reacts with the $SiO_2$. Analysis of the Mn $L_{23}$ intensity ratio in the EELS spectra indicates that the chemical composition in the barrier region which has a measured thickness of 2.6 nm is $MnSiO_3$.  [http://dx.doi.org/10.1063/1.4822441]



Conventional bilayers of Ta/TaN barriers layers[1,2] deposited using physical vapour deposition (PVD) are currently employed in the semiconductor industry to prevent the interdiffusion of copper interconnects and the surrounding insulating dielectric materials. Deposited diffusion barrier layers exist at the expense of the cross-sectional area and consequently increase the resistance of Cu interconnects.[3] Hence, the thickness of this bilayer region must be minimised in order to prevent an increase in interconnect resistance. However, due to the PVD "shadowing" effect, Ta/TaN layers of this thickness often suffer from poor step coverage on the sidewalls and bottom corners of trenches and vias. Hence, to achieve the minimum barrier layer thickness required for future technological nodes proposed by the International Technology Roadmap for Semiconductors,[4] an alternative to Ta/TaN must be found which offers resistance to Cu diffusion, low electrical resistivity, and compatibility with conformal deposition techniques.

Recently, self-forming diffusion barriers have been proposed by various research groups as a promising method of incorporating barrier layers into future interconnect technologies. The process involves the deposition of a Cu/metal alloy directly onto the dielectric, which upon anneal results in the expulsion of the alloying element to the dielectric interface where it chemically reacts to form a diffusion barrier. Mn,[5,6] Ti,[7] and Al[8] have been shown to be suitable alloying elements and to be effective at preventing Cu diffusion into the dielectric material.

On the other hand, the continued reduction in transistor size has led to an increase in on-chip interconnect RC delay, which is directly related to the dielectric constant of the surrounding insulating material.[9] Therefore, one of the primary targets for interconnect research is the integration of self-forming Cu diffusion barrier layers with porous low dielectric constant SiOC:H based materials.[10] Recent studies have shown that the formation of Mn silicate barriers on carbon doped low-$\kappa$ dielectrics can result in the removal of carbon from the dielectric,[11] while the use of porous low-$\kappa$ materials can result in the integration of gaseous Mn precursors within the dielectric pore structure.[12] As such, investigating the formation of Mn based self-forming barrier layers on $SiO_2$ in this paper is intended to act as an important base line study before investigating the more complex Mn/SiOC:H interface.

 

To date, the characterization of the structural and chemical nature of the self-formed diffusion barrier layers using transmission electron microscopy (TEM) and related analytical techniques has been carried out mainly in conventional TEM and high resolution TEM modes after the barrier formation process is complete. Even though these techniques can provide excellent results and in many cases are sufficient to answer some fundamental questions, the nature of the image formation cannot reveal many important aspects of the barrier layer formation process, and complementary techniques are required. For example, due to the amorphous structure of the diffusion barrier formed, it is difficult to unambiguously distinguish the barrier layer from the $SiO_2$ layer which is also amorphous. Therefore, precise measurements of barrier layer thickness or even the exact location (whether it was formed in the alloy matrix or in the $SiO_2$) cannot be made. In the same way, the spatial resolution that can be achieved for chemical analytical techniques is not comparable to that obtained when a convergent beam is used. This may be the reason for the sparse and somewhat contradictory information found in the literature regarding the exact nature and composition of these barriers.[5,6,13]

Scanning transmission electron microscopy in high angle annular dark field mode (STEM-HAADF) is a powerful technique based on the fact that the contrasts in the images are proportional to the atomic number of the species present. Therefore, it allows for the direct visualization of composition variation as a result of phase transformations or chemical reactions that could take place, which is not possible with conventional TEM. In addition, in the STEM-HAADF configuration, complementary analytical techniques, such as energy dispersive X-ray spectroscopy (EDX) or electron energy loss spectroscopy (EELS) can be performed, with greatly improved spatial resolution.

In this study, we investigate the formation and composition of self-forming diffusion barrier in Cu(Mn) alloys using STEM based imaging and analytical techniques with sub-nanometric resolution. The composition of the Cu(Mn) layer and the interfacial barrier layer region are analyzed both before and after *in situ* annealing, while the chemical nature of the Mn in the different layers is also investigated. Cu(Mn) alloys were deposited at room temperature on a thermally grown amorphous 5.4 nm $SiO_2$ layer on a silicon substrate using an Oxford Applied Research EGC04 mini electron-beam evaporator, at a chamber pressure of $5 \times 10^{-9}$ mbar. Samples were studied before and after *in situ* high temperature annealing in a heating holder attached to a 4000SE electron microscope. STEM-HAADF, EDX spectroscopy, and EELS in STEM mode measurements were carried out on a JEOL3000 FEG microscope operating at 300 kV. Samples in cross section geometry were prepared by the conventional method of grinding and polishing followed by $Ar^+$ milling in a Gatan PIPS until electron transparent.

A low magnification STEM micrograph (Figure 1(a)) of the 170 nm thick Cu(Mn) alloy layer displays good uniformity and a sharp interface with the $SiO_2$. EDX spectra averaged over different areas of the un-annealed sample indicate a homogenous composition of ∼10% at. Mn concentration. The high resolution HAADF micrograph of the sample before annealing, shown in Figure 1(b) displays an abrupt alloy/$SiO_2$ interface indicative of no interactions between the alloying metals and the $SiO_2$ layer. Since the micrographs show the silicon lattice atomically resolved, it is possible to accurately calibrate the thickness of the $SiO_2$ layers, which was measured to be 5.4 nm prior to annealing.

The TEM sample was then annealed in sequential steps of 30 min duration at 250 °C, 300 °C, and 350 °C. After the annealing, it was again analyzed with the same techniques and under the same conditions as those used for the untreated sample. Figure 1(c) clearly shows the formation of an additional layer with a thickness of ∼2.6 nm located at the interface between the $SiO_2$ and the alloy after the consecutive set of anneals. The reduced contrast of this region in the HAADF micrograph suggests its elemental composition has a higher average atomic number than $SiO_2$. Additionally, the thickness of the $SiO_2$ has been reduced to 3.4 nm which confirms that this interfacial layer has been formed at the expense of reducing the total thickness of the dielectric or, in other words, it has been formed in the $SiO_2$ layer.

The composition of the different layers before and after annealing was also investigated by EELS in STEM mode. The inset in Figure 1(a) shows two EELS spectra immediately above and below the alloy/$SiO_2$ interface confirming again its abrupt nature. To investigate changes in the

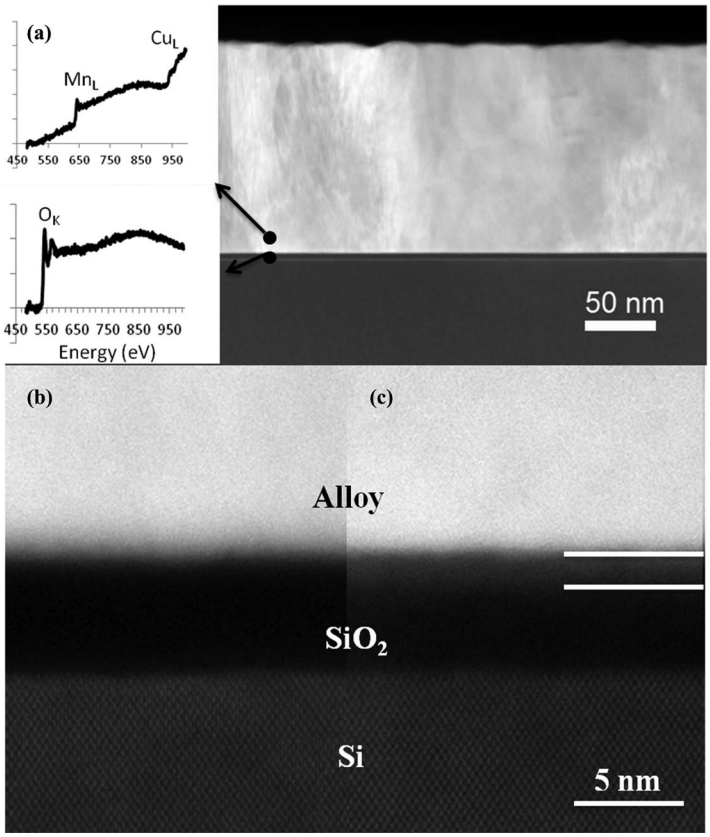


FIG. 1. (a) Low magnification HAADF micrograph of the Cu (Mn) alloy before annealing. In the inset, EELS spectra immediately above and below the alloy/$SiO_2$ interface. High resolution HAADF micrographs of the Cu(Mn) alloy (b) as deposited and (c) after the sequential annealing where a new layer has been formed at the alloy/$SiO_2$ interface as highlighted by the white horizontal lines.

sample after annealing, linescans across the whole structure and particularly across the newly formed layer were recorded with a nominal probe size of 0.5 nm. The Si *K*, Mn *L*, and O *K* signals were extracted after background subtraction and multivariate statistical analysis noise reduction, with the remaining signal under the corresponding peaks being integrated. Fig. 2 shows that Mn has been expelled from the copper migrating mostly to the interface with the $SiO_2$, while some has also diffused to the surface, in agreement with a recent publication.[14] The extracted O K edge signal profile follows a similar intensity trend to that of Mn, while the Si K edge drops rapidly in the alloy layer. It should be noted that the Si background signal has been attributed to the distribution of Si atoms across the sample surface during the milling procedures used during sample preparation. Significantly, no trace of copper is found in the residual dielectric layer. At the temperature of 350 °C, interdiffusion between Cu and Si would normally occur,[15] which indicates that the newly formed interfacial region acts as an effective barrier to Cu diffusion following thermal annealing.

Finally, the nature and chemistry of the different manganese species in the layers was investigated. In order to determine the oxidation state of Mn, the Mn $L_{23}$ intensity ratio was estimated, which is the most widely reported method used in the literature. In this case, a Hartree Slater step function was applied to take into account thickness effects (see Figure 3). The continuum intensity was normalized to the original spectra using a scaling window of 2 eV placed immediately after the L2 peak. The remaining intensity in the white lines was integrated over a 4 eV window centered at the peak maxima, and the obtained values for the $L_3/L_2$ intensity ratio were compared with the values reported by Schmidt *et al.*[16] and correlated with the Mn oxidation state. The EELS spectrum taken from the Mn that has been expelled to the surface, shown in Figure 3 has an average value of

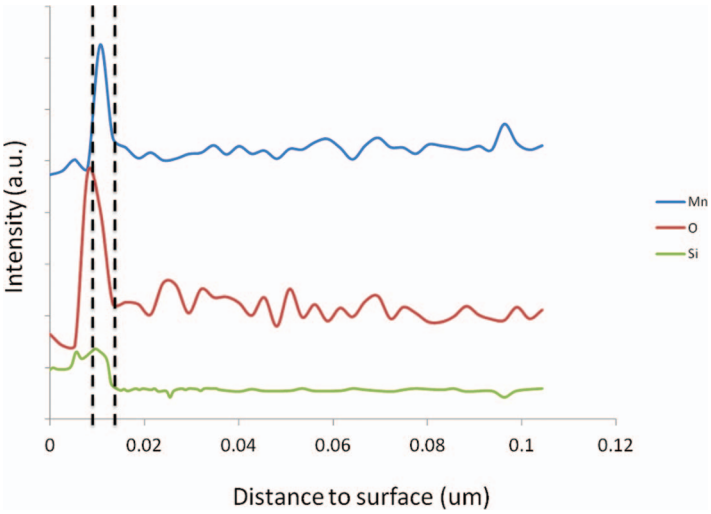


FIG. 2. EELS extracted composition profiles for Mn, O, and Si across the different layers. The area corresponding to the self-formed diffusion barrier is shown between dashed lines.

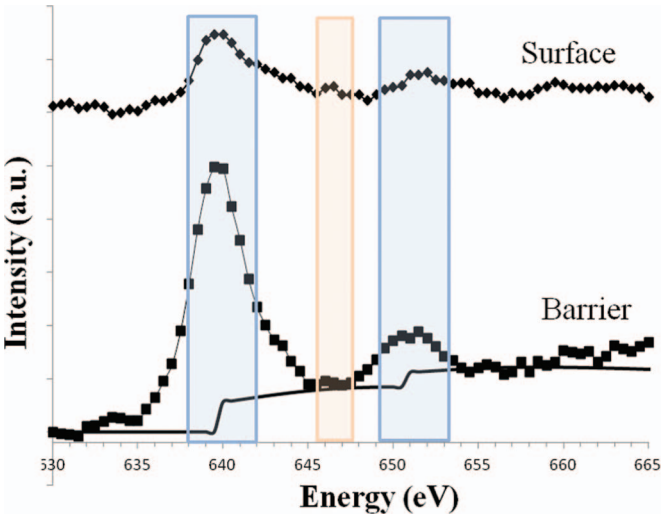


FIG. 3. EELS spectra of the Mn L edge at the surface of the alloy layer and in the barrier region at the $SiO_2$. Shaded in orange is the scaling window used to normalize the continuum intensity and shaded in blue, the windows used to integrate the signal under the $L_2$ and $L_3$ edges.

I ($L_{23}$) = 3.4 ± 0.3, which corresponds to Mn almost entirely in a +2 oxidation state, i.e., MnO. The presence of other residual manganese oxides ($Mn_3O_4$, $MnO_2$, or $Mn_2O_3$) cannot be ruled out but their influence on the calculated intensity ratio in terms of decreasing its value is minimal. For the diffusion barrier region, the average calculated intensity ratio is I ($L_{23}$) = 4.3 ± 0.4. This would correspond to Mn in a purely +2 oxidation state. Given the composition profiles observed (Mn, Si, and O in the self-formed diffusion barrier region), it is suggested that the barrier is primarily composed of $MnSiO_3$, which is in good agreement with the composition recently reported by Casey *et al.*[17] for annealed ultrathin layers of pure metallic Mn on $SiO_2$.

The activity coefficients of Mn in Cu, especially for low concentrations, has been reported to be larger than unity,[18] which means that the solute atoms in the Mn(Cu) alloy will be expelled from the matrix if a more favorable chemical reaction can take place. This is confirmed by the observation of Mn migrating to the surface of the alloy to react with residual oxygen present during the annealing to form MnO, via the displacement reaction $Cu_2O + Mn \rightarrow MnO$, which is in agreement with

the composition observed in that location. While the presence of this layer of MnO at the surface may cause an increase in resistivity which would be detrimental for the final performance of the interconnect, it can be easily removed by polishing techniques leaving almost pure Cu as reported by Iijima *et al.*[19] In the same way, these results suggest that annealing at a temperature less than 350 °C causes the migration of Mn to the $SiO_2$/alloy interface where it subsequently reacts to form a new stable layer consistent with a Mn silicate composition $MnSiO_3$, in agreement with previous studies.[17]

In summary, HAADF, EDX, and EELS in STEM mode were used to characterize Cu(Mn) alloys deposited on $SiO_2$ with a sub-nanometric spatial resolution. The deposition process does not involve any interdiffusion or reaction at the interface between the alloy and the dielectric within the detection limits of the techniques used. However, EELS spectra taken after annealing show that Mn diffuses to the Mn/$SiO_2$ interface and reacts to form a $MnSiO_3$ layer with a measured thickness of 2.6 nm. It should be clearly noted that these results suggest that the $MnSiO_3$ barrier layer can be formed following thermally annealing at temperatures below 350 °C. This may be of considerable technological relevance given that it is essential to limit the total thermal budget employed during backend interconnect processing. Results suggest that Mn is also expelled to the surface of the Cu(Mn) alloy and forms the Mn oxide species MnO through interaction with ambient oxygen. EELS spectra taken following the 350 °C anneal show no evidence for the presence of Cu within the $SiO_2$ substrate suggesting the $MnSiO_3$ layer is an effective barrier to Cu diffusion at this temperature.

J. G. Lozano would like to acknowledge the support of the European Commission under the Marie Curie Programme 2009. Financial support from the SFI PI programme Science under Grant No. 08/IN.1/I2052 is also acknowledged.

[1] A. E. Kaloyeros and E. Eisenbraun, Annu. Rev. Mater. Sci. **30**, 363 (2000).
[2] J. S. Reid, E. Kolawa, R. P. Ruiz, and M. A. Nicolet, Thin Solid Films **236**, 319 (1993).
[3] J. Koike and M. Wada, Appl. Phys. Lett. **87**, 041911 (2005).
[4] *International Roadmap for Semiconductors, 2011 ed., Interconnects*, p. 2.
[5] J. Koike, M. Haneda, J. Iijima, Y. Otsuka, H. Sako, and K. Neishi, J. Appl. Phys. **102**, 043527 (2007).
[6] J. M. Ablett, J. C. Woicik, Zs. Tokei, S. List, and E. Dimasi, Appl. Phys. Lett. **94**, 042112 (2009).
[7] K. Kohama, K. Ito, Y. Sonobayashi, K. Ohmori, K. Mori, K. Maekawa, Y. Shirai, and M. Murakami, Jpn. J. Appl. Phys. **50**, 04DB03 (2011).
[8] D. C. Perng, J. B. Yeh, K. C. Hsu, and S. W. Tsai, Thin Solid Films **518**, 1648 (2010).
[9] N. M. Phuong, Y. Sutou, and J. Koike, J. Phys. Chem. C **117**, 160 (2013).
[10] N. Jourdan, Y. Barbarin, K. Croes, Y. K. Siew, S. Van Elshocht, Z. Tokei, and E. Vancoille, ECS Solid State Lett. **2**, P25 (2013).
[11] P. Casey, J. Bogan, and G. Hughes, J. Appl. Phys. **110**, 124512 (2011).
[12] J. Borja, J. L. Plawsky, W. N. Gill, H. Bakhru, M. He, and T. M. Lu, ECS J. Solid State Sci. Technol. **2**, N175 (2013).
[13] Y. Otsuka, J. Koike, H. Sako, K. Ishibashi, N. Kawasaki, S. M. Chung, and I. Tinaka, Appl. Phys. Lett. **96**, 012101 (2010).
[14] J. G. Lozano, S. Lozano-Perez, J. Bogan, Y. C. Wang, B. Brennan, P. D. Nellist, and G. Hughes, Appl. Phys. Lett. **98**, 123112 (2011).
[15] S. H. Corn, J. L. Falconer, and A. W. Czanderna, J. Vac. Sci. Technol. A **6**, 1012 (1988).
[16] H. K. Schmid and W. Mader, Micron **37**, 426 (2006).
[17] P. Casey, J. Bogan, J. G. Lozano, P. D. Nellist, and G. Hughes, J. Appl. Phys. **110**, 054507 (2011).
[18] R. W. Krenzer and M. J. Pool, Trans. Metall. Soc. AIME **245**, 91 (1969).
[19] J. Iijima, Y. Fujii, K. Neishi, and J. Koike, J. Vac. Sci. Technol. B **27**, 1963 (1963).